Industrial Engineering Journal
ISSN: 0970-2555
Volume : 49, Issue 7, No. 1, July : 2020

A RESEARCH ON THE DESIGN OF A LOW POWER, BETTER WRITE ABILITY SRAM FOR SPACE APPLICATIONS

P.Narasimha Swami, P.Sravan Kumar Reddy, Sk Jakeer Hussain, Dept of Electronics and Communication Engineering, Sree Venkateswara College Of Engineering, Nellore (Dt), Andhra Pradesh, India.
I. Shalini, Dept of Computer Science and Engineering, Sree Venkateswara College Of Engineering, Nellore (Dt), Andhra Pradesh, India.

ABSTRACT
SRAM (Static Random Access Memory) Cells for sophisticated space applications must have great performance to keep up with the space systems' constantly rising data rates and must be radiation-hardened to guarantee dependable operation in severe environments. The SRAM memory cell's functioning is comparatively simple. The Word Line(WL) permits access to the SRAM cell. This regulates the two access control transistors that decide whether or not to link the cell to the Bit Lines (BL).Both read and write operations transfer data using these two lines. In an SRAM cell, there are three operational modes. SRAM cells frequently need to be less energy-hungry and should perform better. Therefore, a new SRAM cell with a higher critical charge and a lower write delay/power is suggested.Due to its lower increased critical charge, the projected DWA12T SRAM cell is appropriate for use in space applications. Hspice was used to execute each design in 16nm technology for a range of supply voltages.

Keywords: SRAM, Stability, Write delay, Read delay, Low leakage power, Soft error issue.

I. INTRODUCTION
There are countless uses for satellite communication. Satellites has a wide range of usage in the modern world, considering weather forecasting, navigational aids, military monitoring, and broadcasting. There is a trend towards producing inexpensive, lightweight satellites as technology advances. [1]. This is so that the cost of producing, deploying, and operating a satellite in orbit, that is compensated by communication sales concluded the course of the satellite's lifespan, is proportional to its mass. great-density memory devices with extended battery lifetimes and the ability to endure severe space radiation are in great demand referable the restricted resources that low-cost satellites may be supplied by SRAM cells are a viable option for space applications because of their high package density and capacity to deliver increased logic performance. [3], [4]. The simplest way to reduce the loss of power to prolong battery life in SRAM cells is by down-scaling supply voltage (VDD). Although reserve power diminishes exponential with VDD whereas dynamic power diminishes quadratic. [5].

But this has a number of negative effects. When the supply voltage is lowered, the SRAM cell change state much sensitized to soft errors, including single-cell upsets (SCUs) and multiple-cell upsets (MCUs), which both affect a number of bits of data. This is because, when susceptible to space electromagnetic waves so much high-energy particles, the critical charge Qc, that is the least assertion needed to flip the data memory in an SRAM cell, falls as V DD. [5]. Additionally, since deep sub-micrometer (DSM) technology develops, line edge texture (LER) and random dopant shifts (RDF) increase the quantity of threshold voltage (Vt) inconsistency among adjacent semiconductors in a memory cell. [6]. Read upset and write occurrence are also more likely imputable the standard 6T SRAM cell's inability to keep in the needed device ratio of strength when process, voltage, and temperature (PVT) fluctuations become greater during (VDD) scaling. [7]. The traditional 6T exhibits half-select disruption as well, which might result in incorrect writing in the unselected cells.

II. STATIC RAM:

Industrial Engineering Journal
ISSN: 0970-2555
Volume : 49, Issue 7, No. 1, July : 2020
Each bit is stored using latches in static random access memory (SRAM), a category of random access memory.
A typical SRAM cell, often known as a 6T SRAM cell, consists of six MOSFETs.
The traditional SRAM design is 6T SRAM. There are six transistors in this, with two of them being PMOS transistors.
The PMOS and NMOS incooperate to category a cross-coupled inverter when the two NMOS transistors are attached in pairs to the bit lines.As a result, these transistors coupled to the NMOS bit lines and controlled through the word line are known as "access transistors".

III.HSPICE TOOL IMPLEMENTATION:

Install the most recent version of the H-Spice programme.Create the licence in the LM tools to run our code after installation.Open a notepad and enter the "netlist code" for the circuit. Save the file with the "filename.sp" extension.Browse the location of the netlist code file in H-spice programme.To simulate the circuit and have H-Spice begin executing our code, click "simulate".To see our output, click "Edit LL". All of the data regarding measurement results, operational points, and error messages are contained in this file.Click "waveview" after making sure there are no problem warnings.Starting now, H-Spice will display the circuit waveforms.

IV.6T SRAM CELL:

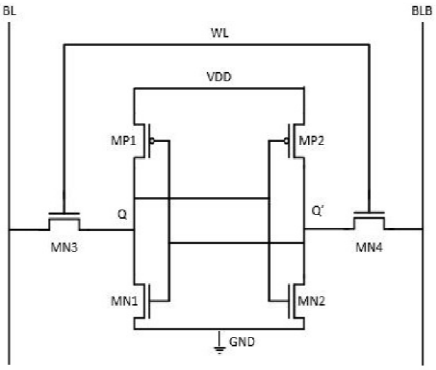

Fig-1: 6T SRAM CELL

READ OPERATION:

This is the situation when a memory cell is being queried for data. The bit line (BL) associated bit line-bar (BLB) are therefore pre-charged to a logic state of 1 (Vdd) whenever the word line (WL = 0) is low. The phrase line (WL) becomes operational (WL = 1) after the pre-charge cycle, causing both access transistors (MN3 and MN4) to switch on and link to the bit lines.

WRITE OPERATION:

A cell is in this condition whenever data is added to or updated in it.The word line, writer enable, and sensing amplifier have to be switched on before writing data into a cell. When they are, the writing driver input pin is used to drive the input information, and the bit line is then dragged to the value of the information provided whereas the bit line bar (BLB) accepts the corresponding value. For example, if $\text{data} = 0, \text{BL} = 0$ and $\text{BLB} = 1$ (Vdd); yet, if $\text{data} = 1, \text{BL} = 1$ (Vdd) and $\text{BLB} = 0$ (gnd).The cell will flip as a result, and the data is effectively written, provided that transistors MP1 and MN3 have the proper sizes. Vdd.

HOLD OPERATION:

because the word line has not been entered, the bit line and bit line bar are broken at gnd while the access control transistors are disconnected, and a cell of SRAM is in this mode when the information is idle (held in the latch).The PMOS transistors will consequently maintain their bond with The data saved in the latch is maintained between them for the duration as they are powered.Figure 1a

illustrates what happens when "1" is kept in the cell within this idle/retention mode. MP1 and MN1 are turned on, which results in positive feedback across the Q and QB nodes, dragging Q to Vddwhile"0" has been saved in the cell, for example, QB is pulled to Vdd while MP1 and MN1 are OFF.

V.RELATED WORKS:

Decoupling inverters are used by the completely differential 8T (FD8T) to lessen half-select disturbance, although this compromises read stability (RSNM).

The single-ended disturb free 9T, which uses singular complete match indication approach to separate their stored nodes by bit-lines during reading operation, is responsible for the advancements in Qcis.

Data-dependent bit line leakage is the effect of this. By utilising a 9T bit-interleaving design, static power dissipation is reduced. Their hold stability has been severely compromised, though. To reduce static power dissipation, the differential 12T (D12T) incorporates a data-dependent leakage control scheme.

Although it increases read security, the WWL12T's power consumption is notably high. Half-select free dynamical loop-cutting write assistance 12T (DWA12T) SRAM is suggested tooptimize read stability and write capability including low power leakage consumption. additionally increase the battery life of memory chips for satellites, this study will suggest an innovative, very energy-efficient SRAM (Static Random Access Memory) Cell.

This New SRAM cell is assumed to achieve a furthermore lower write delay, read delay and advanced the stabilities of read, write and hold modes of operation, to mitigate the soft error issues, compared to that of previously proposed FED8T/9T/D12T/DWA12T under severe process and various temperature conditions.

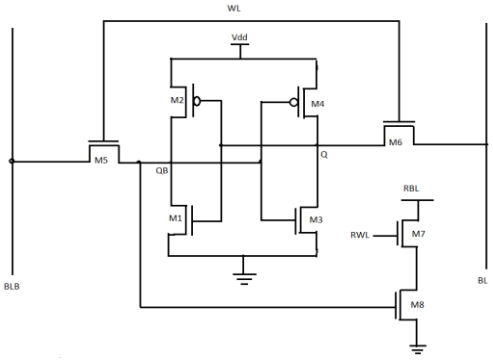

Fig-2: 8T SRAM CELL

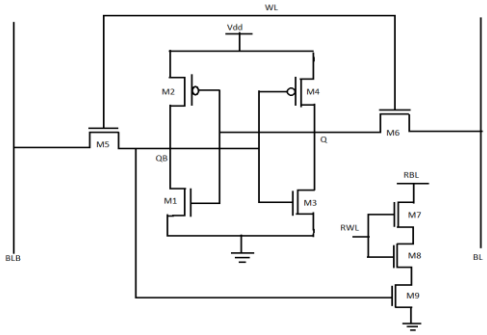

Fig-3: 9T SRAM CELL

Industrial Engineering Journal
ISSN: 0970-2555
Volume : 49, Issue 7, No. 1, July : 2020

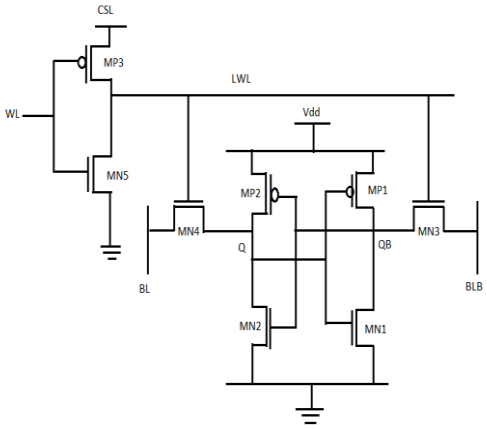

Fig-4: FD8T SRAM CELL

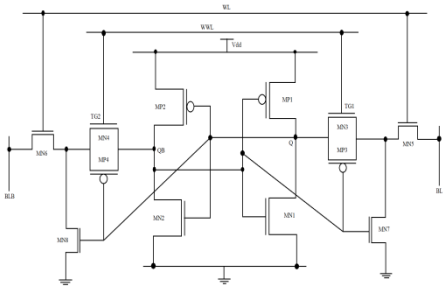

Fig-5: WWL12T SRAM CELL

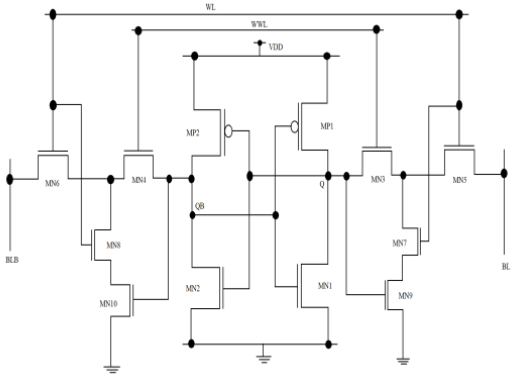

Fig-6: D12T SRAM CELL

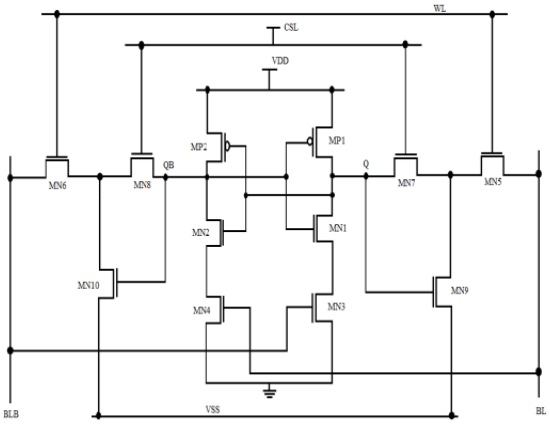

Fig-7: DWA12T SRAM CELL

Industrial Engineering Journal
ISSN: 0970-2555
Volume : 49, Issue 7, No. 1, July : 2020

VI. PROPOSED DWA12T (PDWA12T) SRAM cell:

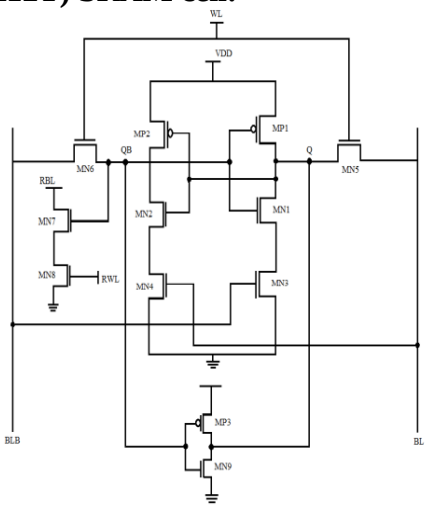

Fig-8: PDWA12T SRAM CELL

Below in fig.(8) is the proposed DWA12T's schematic circuit diagram. The bit lines BL and BLB regulate the word line (WL), that turns on the access transistors MN5 and MN6. The depository nodes Q and QB are separated from one another by a third CMOS inverter. Pull-down transistors MN1/MN2 are coupled in series with two more NMOS transistors, MN3/MN4, which are controlled by BLB/BL. Separate control signals RWL and RBL, which are connected at storage node QB, are used to access the other two transistors MN7 and MN8, respectively.

Write operation:

In order for the approach transistors MN5 and MN6 to turn on, the word line (WL) has been activated in the write operation. The bit lines BL/BLB are either retained at VDD/GND or GND/VDD calculate on whether "1"/"0" *or* "0"/"1" is to be in writing to storage node "Q"/"QB". Assume that the storage node Q will receive the case Write-1, or the number "1". The impulsive loop-cutting transistor MN3 is off and MN4 is on in this scenario because BL is at VDD and BLB is at GND. There is no access to the GND on the right side since MN3 is off. As a result, the pull-up strength rises and the pull-down strength decreases. However, the pull-down power on the left side is unchanged. As the pull-up strength increases, it becomes easier to write '1' into the keeping node 'Q', in turn, quickens the write operation. This process is vice-versa for write-0 operation.

Read operation:

There are distinct bit lines and word lines, or RBL and RWL, in this proposed DWA12T SRAM cell. Assertion the bit line RBL to high (VDD) first, then carry out the read operation. To turn on the transistor MN8, the word line RWL must remain high (VDD). WL and BL/BLB control signals were also deactivated. RBL or BL/BLB discharges to the ground depending on which of either 'Q' or 'QB' holds the data '1' or '0'. Assume the following: The data '0' is to be read from the storage node 'Q' in a read-0 operation. Since "Q" is "0,""QB" will be "1." Additionally, when RWL and RBL are maintained at high levels, a discharge path through the transistors MN7 and MN8 leads to the GND. Between the bit lines, there is a sense amplifier (not pictured) attached, which measures the voltage difference between them. Thus, the read-0 operation is finished. The read-1 operation is the reverse of this procedure.

Hold operation:

By connecting the word line (WL), RBL, RWL, and GND to GND, all access transistors are disabled during the hold operation. In order to ensure that just the driver transistors are present and that the loop-cutting transistors MN3 and MN4 are turned on, the bit lines BL and BLB must be kept high. As a result, the held data will be kept in operation.

	Write(0 or 1)	Hold	Read
WL	0	1	0
RBL	1	0	1
RWL	1	0	1
BL	0/1	1	1
BLB	1/0	1	1

Fig-9: Proposed DWA12T Truth table

Dynamical Loop-Cutting Write Assistance process:
The CSL and WL variables were respectively set to VDD to start writing. At VDD, VSS is stored. BL/BLB will continue to operate at VDD/GND or GND/VDD depending on either "1" ("0") or "0" ("1") is to be transmitted to storage node "H" ("L"). Suppose "1" requires to be composed to the "0" retaining node "H." In this case, the dynamic loop-cutting transistor MN3/MN4 can be switched on or off since BL/BLB is at VDD/GND. The straight core inverter is disconnected from GND while MN3 is off. The inverter's pull-down capability is decreased but its pull-up intensity is increased as a result, resulting in it simpler to write "1" to "H." On the other hand, the left-side core inverter's pull-down strength is unaffected. The extra charging line from VSS (maintained at VDD) first interferes with writing because the "1" storing node "L" briefly switches MN10 on. However, MN10 is turned off as the voltage at "L" decreases. On the other hand, the "0" holding node "H" initially disables MN9. The writing operation is accelerated, though, when the voltage at "H" rises because MN9 is activated and a second charging channel from VSS (maintained at V DD) is created. The procedure for writing "1" is now finished. The flexible loop-cutting strategy takes over as the main writing process because a beneficial additional charging path cancels out the effects of a detrimental extra recharging path. The process for writing "0" is identical.

Small indefinite amount Differential Read Method:
Because BL and BLB are presently heavily filled when the reading process starts, and VSS is set to GND. For the purpose of to activate MN5 and MN6, WL is held at VDD. To maintain the archive node "H"/"L"'s separation over BL/BLB, CSL remains at GND. No matter whatever value "H" ("L") stores—"1" ("0") or "0") ("1")—BL or BLB discharged by reading memory MN9 or MN10 to GND. The bitlines are linked to the inputs of a detection amplifiers (not illustrated), and the read operation is completed if the discovers a 50 mV voltage distinction among it.

VII.REPRESENTATION SETUP AND CONSEQUENCE:
Major pattern parameters for the projected DWA12T cell isanalyzedby utilizing the 16-nm CMOS predictive subject kind (PTM) [19] and HSPICE. The suggested cell is contrasted by various modern designs, including the 6T, 8T, FD8T, 9T, WWL12T, D12T, and DWA12T cells, as of the assess its relative presentation. Given that transistor sizing is a key factor in determining how SRAM cells behave, the proper sizing has been assigned to each cell. The DSM technology node has substantial process variation, thus its effects have been taken into account by using the same simulation.
WRITE DELAY:
According to [17], it appears that an estimation of the write delay or access to write duration for writing "1" to "0" memory node "H" was made. Comparing the DWA12T cell with other similar cells at various V DDs, it is clear that it has the longest write capabilities. This is the reason the LWL

is driven from the WL using a second column-decoupling nMOS, MN9. This lessens the LWL swing, which in turn lessens the ability to access transistor's driving power [5]. Because of its single-ended asymmetrical analyzing system and longer TWA compared to other asymmetrical writing cells, the 9T cell can be difficult to write the number "1" to.The additional TGs in the entry channel that update the data stored inside the storage nodes and slow down the writing process lead the WWL12T cells to show a larger write delay compared to the DWA12T and D12T cells. Due to the use of a dynamic loop-cutting writing approach, the recommended DWA12T cell has a much lower TWA than D12T. However, the FD8T cell shows a 1.37 shorter TWA than the design that was suggested because there are no series-connected accessibility transistors in the entry path.

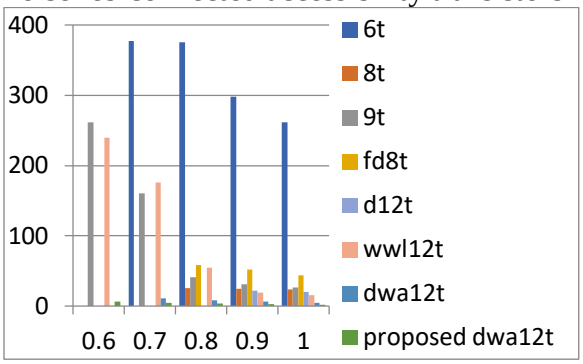

Fig-10: Write-1 Delay bar graph

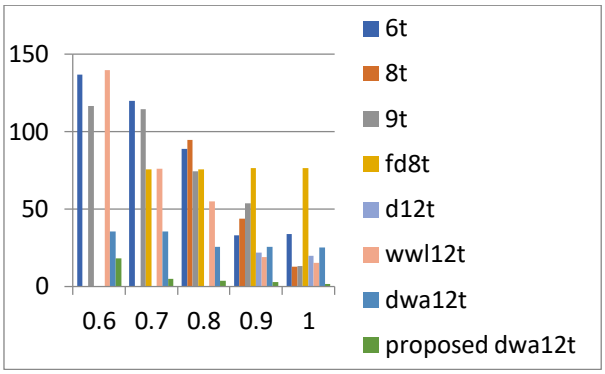

Fig-11: Write-0 Delay bar graph

READ DELAY:

The estimated read access time (TRA) for cells with dual-bit line design is the amount of time needed to reach a 50-mV voltage difference across the two bit lines following WL activation. To allow for fair comparison, the time needed to release the bit line by 50 mV above its initially per-charged value (VDD) after WL activation is used to calculate the TRA of single-ended read cells. The 8T displays the highest TRA among the different comparative cells with different VDD levels because of increased bit line capacitance caused by the combined utilization of bit lines by accessible transistors and read buffers. Due to the same read pathways of the 9T and D12T cells, their TRA is comparable. DWA12T and WWL12T exhibit shorter TRA than 9T/D12T because they share the identical read route, that contains of two transistors as opposed to three read transistors in the 9T/D12T cell. The FD8T exhibits the shortest TRA due to its optimal ratio and 6T-like shape.

Industrial Engineering Journal
ISSN: 0970-2555
Volume : 49, Issue 7, No. 1, July : 2020

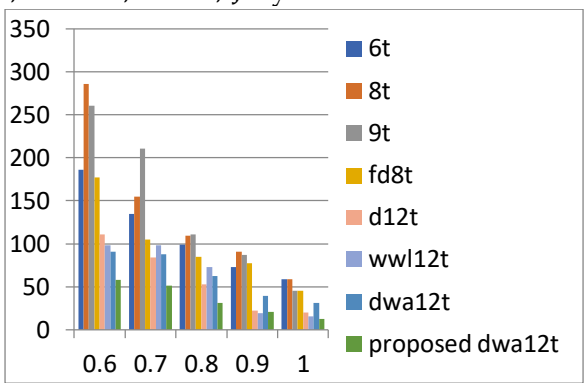

Fig-12: Read Delay bar graph

AVERAGE POWER :

electricity consumption is a key factor in modern technology that determines how much electricity may be used and how efficiently. For greater efficiency, we employ two word lines—w1 and w2—instead of just one, as in the regular 6T SRAM.

The average power is lowered by 90% when comparing the Basic SRAM and the better SRAM, and by 21% among the 8T SRAM and the enhanced SRAM. So, in the interim, that we can use this approach to maximize energy utilization and enhance circuit SNM. We may even decrease power consumption and broaden the possibilities for this circuit by improving scalability. As a result, by rendering unneeded parts inactive, it is feasible to get less average power out of the basic circuit.

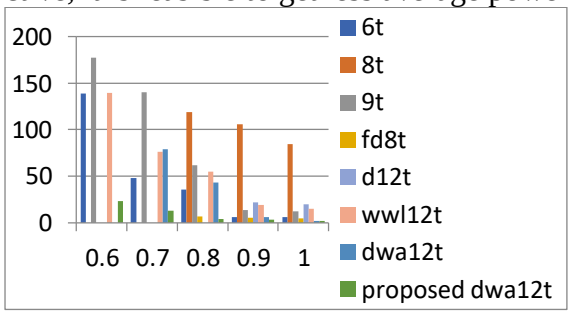

Fig-13: Write-1 Average Power bar graph

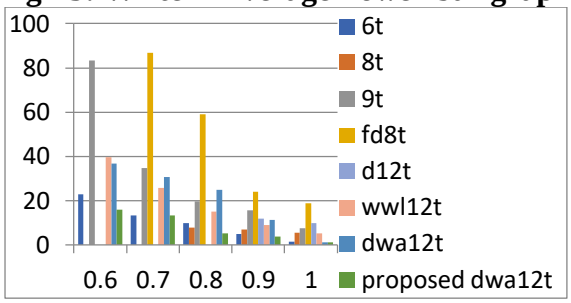

Fig-14: Write-0 Average Power bar graph

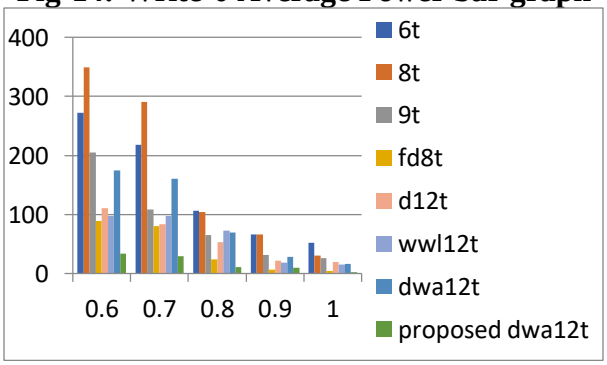

Fig-15: Read Average Power bar graph

Industrial Engineering Journal
ISSN: 0970-2555
Volume : 49, Issue 7, No. 1, July : 2020

CRITICAL CHARGE:

A space-operating SRAM cell is very vulnerable to soft mistakes. The smallest quantity of assertion required to undo the data in a cell and create a soft mistake is noted as the quibbling charge (Qc), which has already been explained in Section I. Since Qc has an exponential relationship in the frequency of soft errors (SER), cells with SRAM that have a greater Qc are less susceptible to SER.The terms Nflux (neutron flux intensity), A (radiation-affected cross sectional area of the storage node), and Qs (device ratio in collecting the charges) are used in this sentence. Qs is normally in fC, hence a small rise in Qc results in a important drop in SER. Utilizing SPICE-based calculations utilizing a double-exponential current supply model, we determined the Qc of the DWA12T cell by comparing it to the Qc of the FD8T SRAM cell.

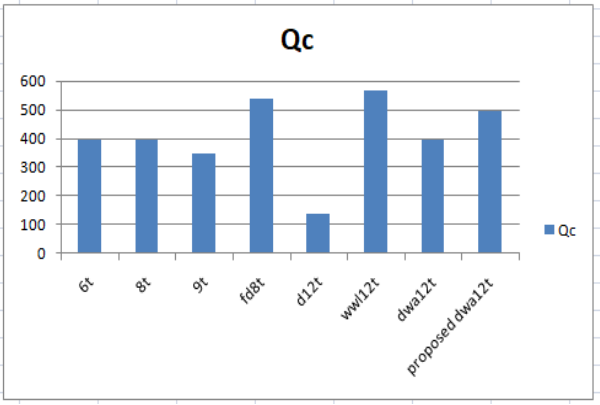

Fig-16: Critical Charge bar graph

COMPARISION TABLE:

	Read Delay (innsec)	Write-0 Delay (innsec)	Write-1 Delay (innsec)	Read Average Power (innWatt)	Write-0 Average Power (innWatt)	Write-1 Average Power (innWatt)	Critical Charge (in ac)
6T SRAM	58.932	33.767	261.496	51.9776	1.57588	5.67687	395.5588
8T SRAM	58.932	12.8776	23.58	29.97868	5.50001	84.46	395.9707
9TSRAM	45.092	13.012	25.969	25.6031	7.4452	11.898	346.0588
FD8T SRAM	45.092	76.4654	43.757	4.2339	18.673	4.7654	537.4925
WWL12T SRAM	15.087	15.087	15.087	15.087	5.087	15.087	568.5504
D12T SRAM	19.966	19.966	19.966	19.966	9.966	19.966	137.6932
DWA12T							397.009

SRAM	31.032	25.2628	4.7866	16.075	1.0533	1.8786	8
PROPOSED DWA12T SRAM	12.0272	1.51487	1.2717	2.4225	1.086	1.8776	495.902

CONCLUSION

This paper discusses a robust, low-power, component-select free DWA12T SRAM cell. The use of an adaptive loop-cutting write aid method considerably improves the proposed cell's write ability and write latency. The decoupling variations-read approach considerably improves read accuracy. The DWA12T cell offers a very low dynamic power consumption since the extra dynamic loop-cutting transistor in the core cell increases the actual channel length and decreases the flow of current from leaking, and VSS is held at V DD throughout idle operation to minimize bit line leakage. The suggested cell displays an astoundingly low sensitivity to soft error regardless of being exposed to strong cosmic rays in space.. In addition, it can use the bit-interleaving construction and is disturb-free due to its half-select design is thus congenial by the usage of suitable ECCs. As a result, the DWA12T is the best option for applications requiring a lightweight, cost-effective cache memory that is both dependable and power-efficient.

REFERENCES

[1] Soumitra Pal, Subhankar Bose, Wing-Hung Ki and Aminul Islam, “Half-Select-Free Low-Power Dynamic Loop-Cutting Write Assist SRAM Cell for Space Applications”, IEEE TRANSACTIONS ON ELECTRON DEVICES, VOL. 67, NO. 1, JANUARY 2020.

[2] Nandakishor Yadav, Ambika Prasad Shah and Santosh Kumar Vishvakarma, “Stable, Reliable, and Bit-Interleaving 12T SRAM for Space Applications: A Device Circuit Co-Design”, IEEE Transactions On Semiconductor Manufacturing, Vol. 30, No. 3, August 2020.

[3] Do Anh-Tuan, Jeremy Yung Shern Low, Joshua Yung Lih Low, Zhi-Hui Kong, Xiaoliang Tan, and Kiat-Seng Yeo, “An 8T Differential SRAM With Improved Noise Margin for Bit-Interleaving in 65 nm CMOS”, IEEE Transactions On Circuits And Systems—i: Regular Papers, Vol. 58, No. 6, June 2018.

[4] Soumitra Pal and Aminul Islam, “9-T SRAM Cell for Reliable Ultralow-Power Applications and Solving Multibit Soft-Error Issue”, IEEE Transactions On Device And Materials Reliability, Vol. 16, No. 2, June 2019.

[5] S. Pal and A. Islam, “9-T SRAM cell for reliable ultralow-power applications and solving multibit soft-error issue,” IEEE Trans. Device Mater. Rel., vol. 16, no. 2, pp. 172–182, Jun. 2016, doi: 10.1109/ TDMR.2016.2544780.

[6] J. P. Kulkarni, K. Kim, and K. Roy, “A 160 mV robust Schmitt trigger based subthreshold SRAM,” IEEE J. Solid-State Circuits, vol. 42, no. 10, pp. 2303–2313, 2007, doi: 10.1109/JSSC.2007.897148.

[7] S. Pal and A. Islam, “Variation tolerant differential 8T SRAM cell for ultralow power applications,” IEEE Trans. Comput.-Aided Design Integr. Circuits Syst., vol. 35, no. 4, pp. 549–558, Apr. 2016, doi: 10. 1109/TCAD.2015.2474408.

[8] D. Anh-Tuan, J. Y. S. Low, J. Y. L. Low, Z.-H. Kong, X. Tan, and K.-S. Yeo, “An 8T differential SRAM with improved noise margin for bit-interleaving in 65 nm CMOS,” IEEE Trans. Circuits Syst. I, Reg. Papers, vol. 58, no. 6, pp. 1252–1263, Jun. 2011, doi: 10. 1109/TCSI.2010.2103154.

[9] L. Wen, Z. Duan, Y. Li, and X. Zeng, "Analysis of a read disturb-free 9T SRAM cell with bit-interleaving capability," Microelectron. J., vol. 45, no. 6, pp. 815–824, Jun. 2014, doi: 10.1016/j.mejo.2014.02.020.
[10] R. E. Aly and M. A. Bayoumi, "Low-power cache design using 7T SRAM cell," IEEE Trans. Circuits Syst. II, Exp. Briefs, vol. 54, no. 4, pp. 318–322, Apr. 2007, doi: 10.1109/TCSII.2006.877276.
[11] S. Pal, V. Gupta, W. H. Ki, and A. Islam, "Transmission gate-based 9T SRAM cell for variation resilient low power and reliable Internet of things applications," IET Circuits, Devices Syst., vol. 13, no. 5, pp. 584–595, Aug. 2019, doi: 10.1049/iet-cds.2018.5283.
[12] S. Gupta, K. Gupta, and N. Pandey, "A 32-nm subthreshold 7T SRAM bit cell with read assist," IEEE Trans. Very Large Scale Integr. (VLSI) Syst., vol. 25, no. 12, pp. 3473–3483, Dec. 2017, doi: 10. 1109/TVLSI.2017.2746683.
[13] N. Verma and A. P. Chandrakasan, "A 256 kb 65 nm 8T subthreshold SRAM employing sense-amplifier redundancy," IEEE J. Solid-State Circuits, vol. 43, no. 1, pp. 141–149, Jan. 2008, doi: 10. 1109/JSSC.2007.908005.
[14] Y. Yang, J. Park, S. C. Song, J. Wang, G. Yeap, and S.-O. Jung, "Singleended 9T SRAM cell for near-threshold voltage operation with enhanced read performance in 22-nm FinFET technology," IEEE Trans. Very Large Scale Integr. (VLSI) Syst., vol. 23, no. 11, pp. 2748–2752, Nov. 2015, doi: 10.1109/TVLSI.2014.2367234.
[15] V. Sharma, S. Vishvakarma, S. S. Chouhan, and K. Halonen, "A writeimproved low-power 12T SRAM cell for wearable wireless sensor nodes," Int. J. Circuit Theory Appl., vol. 46, no. 12, pp. 2314–2333, Dec. 2018, doi: 10.1002/cta.2555.
[16] M.-H. Tu et al., "A single-ended disturb-free 9T subthreshold SRAM with cross-point data-aware write word-line structure, negative bit-line, and adaptive read operation timing tracing," IEEE J. Solid-State Circuits, vol. 47, no. 6, pp. 1469–1482, Jun. 2012, doi: 10.1109/JSSC.2012.2187474.
[17] A. Islam and M. Hasan, "Leakage characterization of 10T SRAM cell," IEEE Trans. Electron Devices, vol. 59, no. 3, pp. 631–638, Mar. 2012, doi: 10.1109/TED.2011.2181387.
[18] S. Ataei, J. E. Stine, and M. R. Guthaus, "A 64 kb differential singleport 12T SRAM design with a bit-interleaving scheme for low-voltage operation in 32 nm SOI CMOS," in Proc. IEEE Int. Conf. Comput. Design, (ICCD), Oct. 2016, pp. 499–506, doi: 10.1109/ICCD.2016. 7753333.
[19] NIMO PTM Model. Accessed: Mar. 2019.
[20] S. Ahmad, M. K. Gupta, N. Alam, and M. Hasan, "Single-ended Schmitt-trigger-based robust low-power SRAM cell," IEEE Trans. Very Large Scale Integr. (VLSI) Syst., vol. 24, no. 8, pp. 2634–2642, Aug. 2016, doi: 10.1109/TVLSI.2016.2520490.
[21] T. W. Oh, H. Jeong, K. Kang, J. Park, Y. Yang, and S.-O. Jung, "Power-gated 9T SRAM cell for low-energy operation," IEEE Trans. Very Large Scale Integr. (VLSI) Syst., vol. 25, no. 3, pp. 1183–1187, Mar. 2017, doi: 10.1109/TVLSI.2016.2623601.
[22] S. Pal, S. Bose, W.-H. Ki, and A. Islam, "Design of power- and variability-aware nonvolatile RRAM cell using memristor as a memory element," IEEE J. Electron Devices Soc., vol. 7, pp. 701–709, Jul. 2019, doi: 10.1109/JEDS.2019.2928830.
[23] S. Pal, S. Bose, W.-H. Ki, and A. Islam, "Characterization of halfselect free write assist 9T SRAM cell," IEEE Trans. Electron Devices, vol. 66, no. 11, pp. 4745–4752, Nov. 2019, doi: 10.1109/TED.2019.294 2493.
[24] E. Grossar, M. Stucchi, K. Maex, and W. Dehaene, "Read stability and write-ability analysis of SRAM cells for nanometer technologies," IEEE J. Solid-State Circuits, vol. 41, no.11,pp.2577–2588,Nov.2006, doi: 10.1109/JSSC.2006.883344.